

Case Report

A Case of Chordoid Meningioma with Allelic Loss of 1p36

Takahiro FUKUDA¹, Takao ARAI², Takashi NIKAI³, Tatsuhiro JOKI², Satoshi IKEUCHI²,
Masataka KATO², Makio KAWAKAMI⁴, and Toshiaki ABE²

¹*Division of Neuropathology, Department of Neuroscience, Research Center for Medical Sciences,
The Jikei University School of Medicine*

²*Department of Neurosurgery, The Jikei University School of Medicine*

³*Department of Pathology, The Jikei University School of Medicine*

⁴*Department of Pathology, Clinical Service, The Jikei University School of Medicine*

ABSTRACT

The unbalanced translocation der(1)t(1;3)(p12-13;q11) with losses of 1p12-13-pter and 3q11-pter has been reported in three cases of chordoid meningioma. Thus far, only a few attempts have been made to analyze this rare variant of meningioma cytogenetically. We report a case of chordoid meningioma in a 68-year-old man. He presented with a large mass in the midline of the base of the frontal skull without surrounding edema and had experienced poor vision with visual field defects and anosmia for 6 months. We investigated the meningioma with fluorescence in situ hybridization and found that the lesion was solid and well-delineated, with low signal intensity on T₁-weighted sequences and high signal intensity on T₂- and proton density-weighted sequences. The tumor showed marked enhancement following gadolinium administration. Histologic examination revealed a tumor composed of trabeculae of eosinophilic vacuolated cells embedded in a myxoid matrix with a focally typical meningiomatous pattern. Electron microscopy revealed intercellular desmosomal junctions and complex cytoplasmic interdigitation. Tumor cells were immunoreactive for vimentin, epithelial membrane antigen, the progesterone receptor, p27, p53, and the epidermal growth factor receptor. Cytogenetic analysis revealed the deletion of 1p36, but not of 1q25, the 3p telomere, the 3q telomere, 10q23, alpha satellite DNA of chromosome 10, the 14q telomere, 19p13, 19q13, 22q11.2, or 22q13. Chromosome 1p36 is a candidate recurrence-associated genomic region in chordoid meningioma. (Jikeikai Med J 2006 ; 53 : 37-44)

Key words : chordoid meningioma, meningioma, fluorescence in situ hybridization, pathology

INTRODUCTION

Chordoid meningioma, first reported in 1980 by Connors¹ and given its present name in 1988 by Kepes et al.², is a comparatively new subtype of meningioma. In their small series of young patients (6 to 19 years old), chordoid meningioma was associated with microcytic anemia or dysgammaglobulinemia (Cast-

leman's syndrome) or both. Couce et al, however, have shown that chordoid meningioma occurs mostly in adults, lacks sex predilection, and has no systemic manifestations³. Although chordoid meningioma accounts for only 0.5% of all meningiomas, it has a high recurrence rate (42% in one series)³. On the basis of its clinical behavior, chordoid meningioma is classified as World Health Organization grade II⁴.

Received for publication, October 20, 2005

福田 隆浩, 荒井 隆雄, 二階堂 孝, 常喜 達裕, 池内 聡, 加藤 正高, 河上 牧夫, 阿部 俊昭

Mailing address : Takahiro FUKUDA, Division of Neuropathology, Department of Neuroscience, Research Center for Medical Sciences, The Jikei University School of Medicine, 3-25-8, Nishi-shimbashi, Minato-ku, Tokyo, 105-8461, Japan.

E-mail : fukuda-t@jikei.ac.jp.

The present case study describes the cytogenetic analysis of a chordoid meningioma using fluorescence in situ hybridization (FISH) and illustrates its cytologic, histopathologic, ultrastructural, and immunohistochemical features.

CASE REPORT

A 68-year-old man complained of visual disturbances lasting 6 months and was referred to our unit after magnetic resonance (MR) revealed an intracranial mass lesion. Physical examination revealed visual acuity of 20/2000 in the left eye and 20/25 in the right eye, superior hemianopsia in the left eye, and anosmia. Results of hematologic examination, including hemoglobin and immunoglobulin, were normal. MR revealed a large, extrinsic mass (6×6×4 cm), extending superiorly to indent both frontal lobes, in the midline of the base of the frontal skull, without surrounding edema. The lesion was solid and well-delineated, with low signal intensity on T₁-weighted sequences and high signal intensity on T₂-weighted and proton density-weighted sequences. The lesion showed marked enhancement following gadolinium administration (Fig. 1). The tumor was supplied by the bilateral ethmoidal arteries and the left maxillary artery. No bone lesion was found.

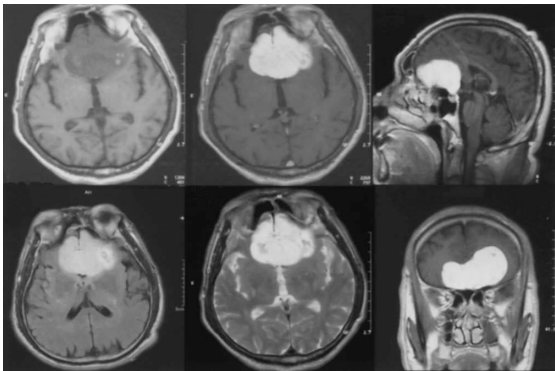


Fig. 1. Brain MR images

A large extrinsic mass (6×6×4 cm), extending superiorly to indent both frontal lobes, was located in the midline of the base of the frontal skull without surrounding edema. The lesion was solid and well-delineated, with low signal intensity on T₁-weighted sequences and high signal intensity on T₂- and proton density-weighted sequences. It showed marked enhancement following gadolinium administration.

The tumor was resected via a bilateral frontal and left frontotemporal approach. With the attachment on the dura of cribriform plate, a well-circumscribed, soft, tan-pink, gelatinous mass was debulked and excised (Simpson Grade II). The patient's postoperative course was uneventful, and visual acuity improved in both eyes. No radiation therapy was administered.

METHODS

Tumor tissue obtained at surgery was fixed in 10% buffered formalin and embedded in paraffin. Sections were stained with hematoxylin-eosin (H & E), periodic acid-Schiff (PAS), Alcian blue, and silver impregnation for reticulin fibers. Immunohistochemical studies were performed with monoclonal and polyclonal antibodies against vimentin, epithelial membrane antigen (EMA; E29; dilution 1:200; DAKO, Glostrup, Denmark), the progesterone receptor (PR; 1A6; dilution 1:800; Novocastra, Newcastle upon Tyne, UK), cytokeratin (CAM5.2; BD Biosciences, San Jose, CA, USA), S-100 (dilution 1:800; DAKO), glial fibrillary acidic protein (GFAP; dilution 1:3000; DAKO), carcinoembryonic antigen (CEA; II-7; dilution 1:50; DAKO), CD31 (JC/70A; dilution 1:50; DAKO), CD34 (My10; dilution 1:50; BD Biosciences), factor VIII (dilution 1:1000; DAKO), collagen type I (dilution 1:20; Southern Biotechnology Associates, Birmingham, AL, USA), collagen type II (dilution 1:20, Southern Biotechnology Associates), collagen type III (dilution 1:100, Southern Biotechnology Associates), collagen type IV, laminin (CIV22; dilution 1:100, DAKO), p53 (DO-7, dilution 1:50, Novocastra), p27 (1B4; dilution 1:20; Novocastra), bcl2 (124; dilution 1:40; DAKO), and the epidermal growth factor receptor (EGFR; EGFR. 113; dilution 1:10; Novocastra). Ulex europeus agglutinin-1 (UEA1) lectin (E.Y. Laboratories, San Mateo, CA, USA) was also used for histochemical studies. The cell proliferative index was calculated according to the percentage of nuclei immunoreactive with the anti-human Ki-67 antibody (MIB-1; dilution 1:500; Zymed Laboratories, San Francisco, CA, USA) in 500 consecutive cells. FISH analysis was

performed with 1p36/1q25, the 3p telomere/3q telomere, PTEN (10q23)/CEP10, the 14q telomere, 19q13/19p13, and TUPLE1 (22q11.2)/ARSA (22q13) dual-color DNA probes (Vysis, Inc., Downers Grove, IL, USA). For each sample, 500 interphase nuclei were evaluated. (If more than 80% of the nuclei showed two green and two red signals, the case was regarded as "normal"; one green or red signal was associated with deletion, and three green or red spots were regarded as duplication.) Specimens obtained from intraoperative touch smear cytology were stained with the Papanicolaou method. Several

small fragments were also fixed with 3% glutaraldehyde and embedded in epoxy resin for ultrastructural study.

PATHOLOGICAL FINDINGS

Microscopic examination showed that the tumor was composed of trabeculae of spindle-shaped and polygonal cells with an eosinophilic cytoplasm (Fig. 2d) and round or oval nuclei with a thin, smooth margin and delicate chromatin (Fig. 2f). Some cells had a physaliferous appearance. The tumor cells

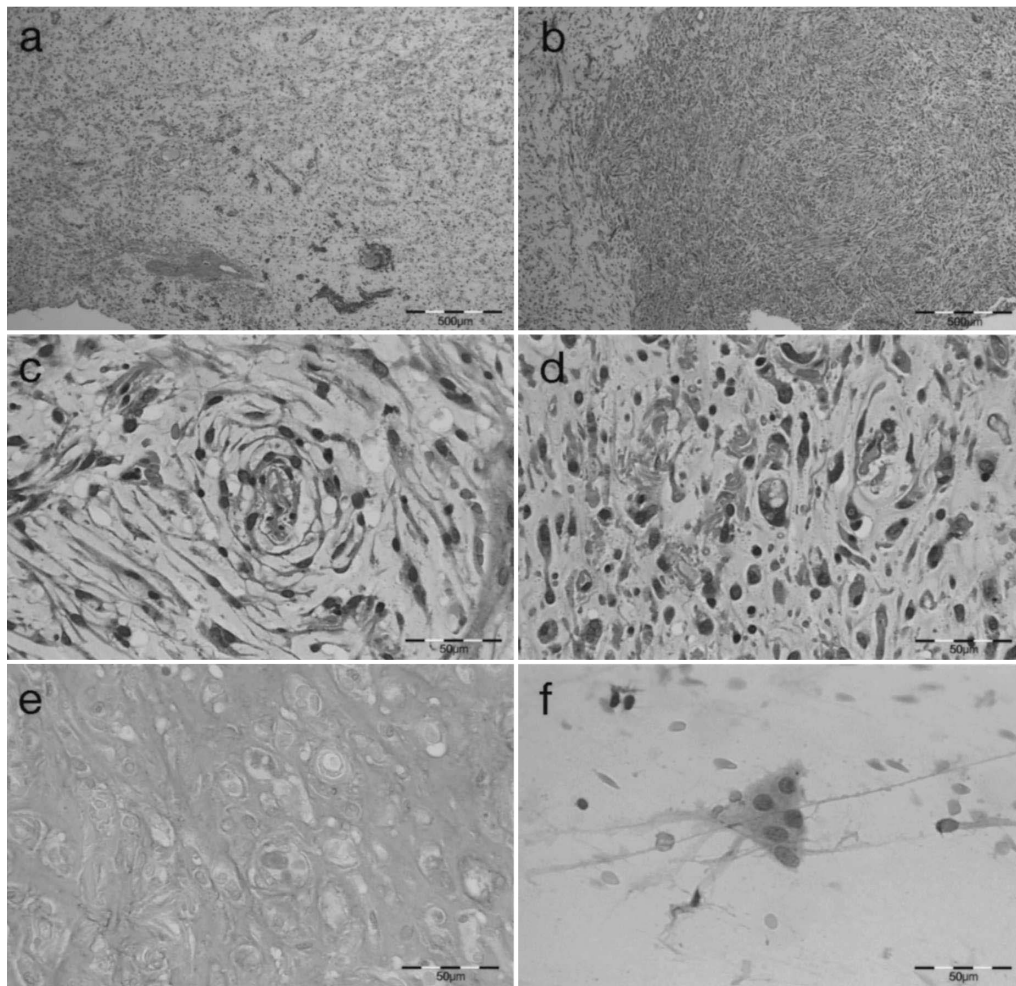


Fig. 2. Microscopic findings

(a) Cordlike arrangement of tumor cells embedded in abundant myxoid matrix (H & E). (b) A classic transitional meningioma pattern with lobular and fascicular arrangements merged at the borders (H & E). (c) Perivascular whorl formation (H & E). (d) Spindle-shaped and polygonal tumor cells with eosinophilic cytoplasm (H & E). (e) Alcian blue-positive mucinous matrices among the tumor cells. (f) Adhesive pseudosyncytial plates composed of medium-sized cells with indistinct cytoplasmic borders on touch smear cytology (Papanicolaou stain)

were embedded in an abundant myxoid matrix, which was basophilic on H & E staining (Fig. 2a), pink with the PAS reaction, and bright blue on Alcian blue staining at pH 2 (Fig. 2e), which is the histochemical pattern of acid mucin. Cytoplasmic vacuolization also exhibited the same staining pattern of the myxoid matrix. There were many small, adhesive pseudosyncytial plates composed of medium-sized cells with indistinct cytoplasmic borders in touch smear cytology (Fig. 2f). Whorl formation (Fig. 2c) and calcification were evident in some areas. No sizable lymphoplasmocytic infiltrate was found. In less than 3% of tumor specimens, a classic transitional meningioma pattern with lobular and fascicular arrangements merging at the borders with very extensive chordoid areas was observed (Fig. 2b).

Ultrastructural study demonstrated cohesive, often polygonal cells, featuring uniform, round-to-oval nuclei with delicate chromatin, as well as moderate quantities of cytoplasm containing abundant rough endoplasmic reticulum, mitochondria, and intermediate filaments. Basement membranes surrounding the cytoplasmic membrane were observed in some areas. Intercellular desmosomal junctions and complex cytoplasmic interdigitation were seen (Fig. 3). Weibel-Palade bodies were not observed.

Immunohistochemical studies of the surgically

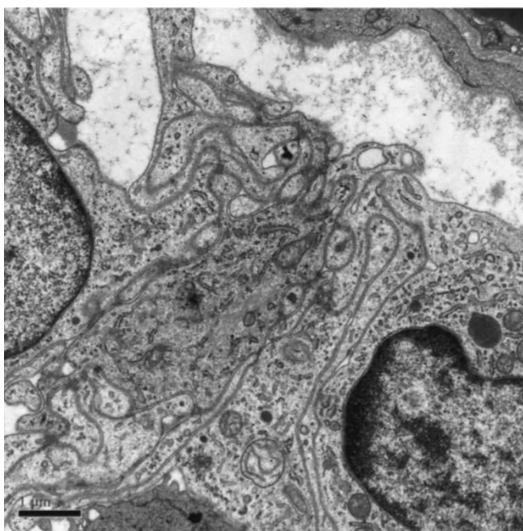


Fig. 3. Electron microscopic findings
Intercellular desmosomal junctions and complex cytoplasmic interdigitation were seen.

resected specimen showed strong, diffuse positivity for vimentin (Fig. 4a), EMA (Fig. 4b), PR (Fig. 4c), and p27 (Fig. 4g) in areas with the chordoid and classic patterns. Some tumor cells expressed p53 (Fig. 4e) and EGFR (Fig. 4f). However, staining was consistently negative for CAM5.2 (Fig. 4d), S-100, GFAP, CEA, CD31, CD34, factor VIII, collagen type I, collagen type II, collagen type III, collagen type IV, laminin, and bcl2. The MIB1 positivity rate (Fig. 4h) was 7% to 14% (mean, 10%).

Cytogenetic analysis revealed the deletion of 1p36, but not of 1q25, the 3p telomere, the 3q telomere, 10q23, alpha satellite DNA of chromosome 10, the 14q telomere, 19p13, 19q13, 22q11.2, or 22q13 (Fig. 5).

DISCUSSION

Most chordoid meningiomas (88%) are large and supratentorial³. The frontoparietal convexities and the parasagittal and falctentorial regions are common sites of origin^{2,3,5}. A large hypointense-to-isointense, dural-based, uniformly enhancing mass and moderate-to-marked adjacent white matter edema are common features on T₁-weighted MR sequences^{5,9}. As in the present report, two previous reports have described chordoid meningiomas as showing high signal intensity in T₂-weighted sequences^{5,6}. Although the authors of these reports have speculated high-intensity intralesional signals reflect, in part, lymphoplasmacytic infiltration, this is not a plausible explanation in the present case.

Cytologic touch smears are a highly reliable diagnostic method for chordoid meningioma^{10,11} and show a pattern of abundant, closely knit plates inside which cellular limits are not visible, with some solitary, rounded cells. Nuclei are homogeneous and display a delicate chromatin pattern with a few conspicuous nucleoli and occasional intranuclear inclusions. The background is a fairly abundant, metachromatic, mucofibrillar matrix that does not appear between the cells inside the plates. Histologic studies show clustering or cords of eosinophilic, vacuolated (chordoid) cells in a myxoid matrix; thus, the histologic appearance of chordoid meningioma may mimic that of chordoma. Typical physaliphorous

tumor cells, however, are absent in chordoid meningiomas. Mucin-rich chordoid elements occupy 10% to 100% of the tumor area³. Perimural and intratumoral lymphoplasmacellular infiltrates, often showing follicles and germinal centers with a predomi-

nance of T-lymphocytes over B-cells, may be prominent in some cases of chordoid meningiomas, particularly those in young patients, and may cause systemic manifestations of Castleman's syndrome². Ultrastructurally, meningiomas have intercellular des-

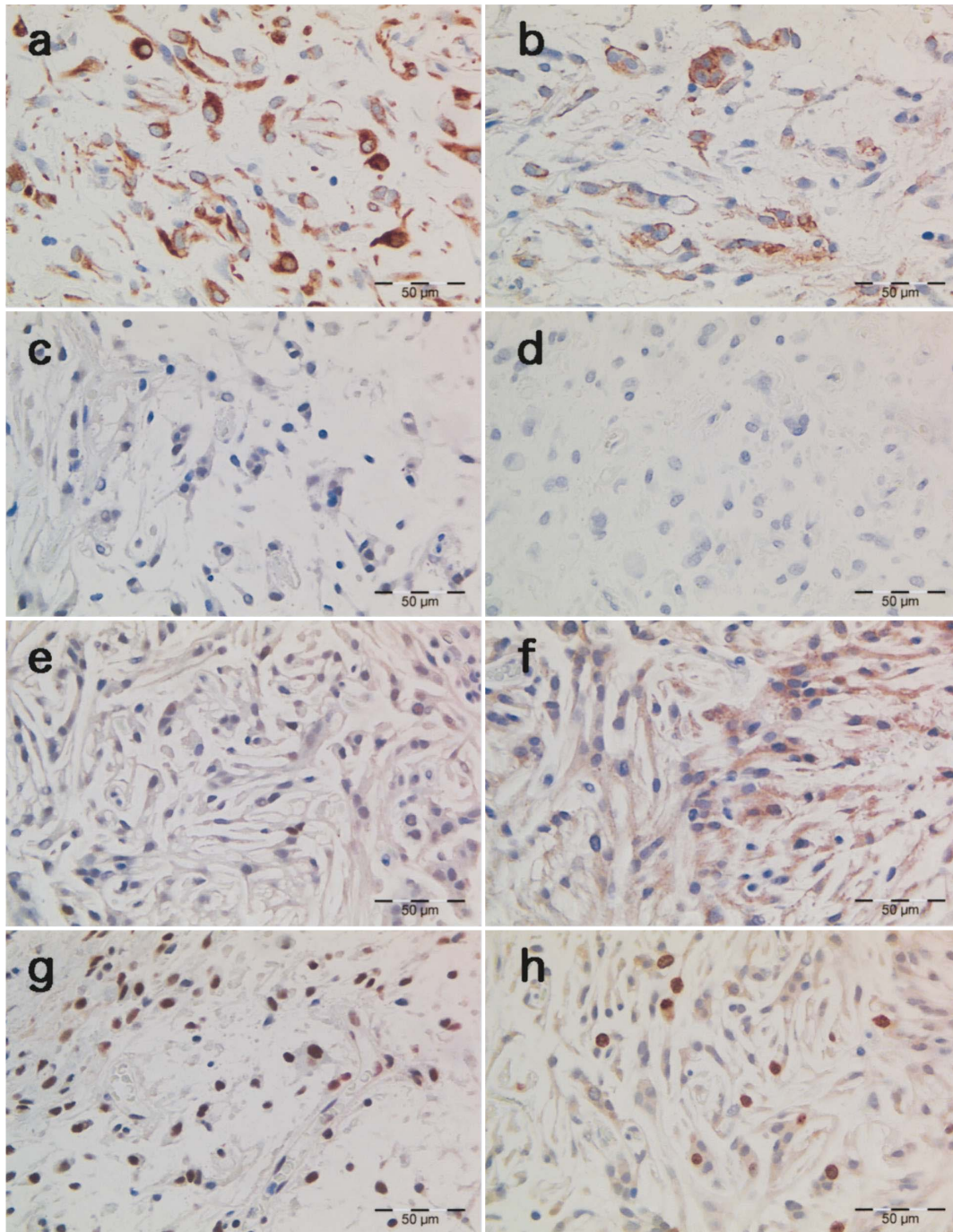


Fig. 4. Immunohistochemical findings
 Positive cytoplasmic staining for vimentin (a) and EGFR (f). Positive membranous staining for EMA (b).
 Positive nuclear staining for PR (c), p53 (e), p27 (g), and MIB1 (h). Negative staining for CAM5.2 (d).

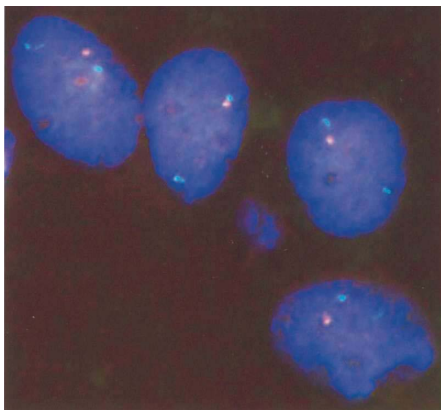


Fig. 5. FISH analysis
Tumor cells showing the deletion of 1p36 (orange)
and a normal number of 1q25 (green).

mosomal junctions, intermediate filaments, and complex interdigitating cell processes, which at times may be difficult to appreciate in the chordoid variant⁵. Almost all tumor cells exhibit positive immunostaining for vimentin, EMA, and PR, but are negative staining for GFAP, S100, cytokeratins, CD34, CD57 (Leu7), and CEA^{3,10,12}. Immunostaining for vimentin and EMA in the absence of prominent cytokeratin expression facilitates the differential diagnosis. In meningioma, MIB1 labeling indices higher than 5% to 10% suggest a greater likelihood of recurrence⁴.

Microscopically, chordoma¹³, chondroid chordoma¹⁴, myxoid chondrosarcoma (chordoid sarcoma)^{15,16}, epithelioid hemangioendothelioma¹⁷, metastatic mucinous carcinoma¹⁸, and chordoid glioma¹⁹ require immunohistochemical and ultrastructural examinations for their differentiation. The present case showed some chordoma-like features with lobules of vacuolated cells and physaliferous-like cells in a myxoid stroma. There were, however, small meningothelial elements in other parts of the tumor that aided the diagnosis of chordoid meningioma. This diagnosis was further supported by the immunoreactivity for vimentin, EMA, and PR and the ultrastructural findings of cytoplasmic interdigitations, desmosomes, and intermediate filaments, which are characteristic of meningioma. Immunohistochemically, chordomas are characterized by S-100 protein and cytokeratins¹³, chondroid chordoma by S-100 protein¹⁴, myxoid chondrosarcoma by cytoplasmic positivity for vimentin, synaptophysin, S-100, and

EMA15, epithelioid hemangioendothelioma by CD31, CD34, factor VIII, and *Ulex europaeus* lectin¹⁷, metastatic mucinous carcinoma by cytokeratin¹⁸, and chordoid glioma by GFAP¹⁹.

A large study of meningiomas has revealed that overexpression of p53 protein correlates with the MIB-1 proliferative index²⁰, histologic malignancy²¹, and recurrence²². In another study, however, no relationship between p53 expression and prognosis was found²³. Suggested roles of nuclear protein p21, a universal cyclin-dependent kinase inhibitor, also differ between studies. Amatya et al. have reported a negative correlation of the proliferative index with the histological grade of meningioma²⁴. On the other hand, Korshunov et al. have found no correlation of p27 with various histologic and clinical outcomes²⁵. EGFR seems to be highly expressed in meningiomas, but its clinical significance has not been established²⁶. Thus, the roles of p53, EGFR, and p21 in meningiomas, especially chordoid meningioma, remain unclear.

Unbalanced translocation der(1)t(1;3)(p12-13;q11) with losses of 1p12-13-pter and 3q11-pter has been reported in three cases of this rare variant meningioma by using chromosome microdissection and reverse FISH²⁷. In this case, FISH analysis revealed deletion of 1p36, but not of 1q25, the 3p telomere, the 3q telomere, 10q23, alpha satellite DNA of chromosome 10, the 14q telomere, 19p13, 19q13, 22q11.2, or 22q13. Deletion of 1p, mainly in the regions 1p36, 1p35-p32, and 1p22-p13, is the most frequent progression-associated chromosomal aberration in meningiomas and is strongly correlated with tumor recurrence^{28,30}. The results of the present case and previously reported cases^{27,31} indicate that chromosome 1p36 is a candidate recurrence-associated genomic region in chordoid meningioma. Atypical and anaplastic meningiomas often show allelic losses of chromosomal arms 1p, 6q, 9q, 10q, 14q, 17p, and 18q and gains of 1q, 9q, 12q, 15q, 17q, and 20q, suggesting the presence of progression-associated genes at these loci^{32,33}. Thus far, only a few attempts have been made to analyze chordoid meningioma cytogenetically. Therefore, further studies are required to demonstrate the clear significance of genetic factors for meningioma biology and clinical outcome.

REFERENCES

1. Connors MH. Growth and maturation arrest, hypochromic anemia and hyperglobulinemia associated with a brain tumor. *West J Med* 1980 : 133 ; 160-3.
2. Kepes JJ, Chen WY, Connors MH, Vogel FS. "Chordoid" meningeal tumors in young individuals with peritumoral lymphoplasmacellular infiltrates causing systemic manifestations of the Castleman syndrome: a report of seven cases. *Cancer* 1988 : 62 ; 391-406.
3. Couce ME, Aker FV, Scheithauer BW. Chordoid meningioma: a clinicopathologic study of 42 cases. *Am J Surg Pathol* 2000 : 24 ; 899-905.
4. Louis DN, Scheithauer BW, Budka H, von Deimling A, Kepes JJ. 2000. Meningiomas. In: Kleihues P and Cavenee WK editors. *Pathology and genetics of tumors of the nervous system*. Lyon: IARC Press; 2000. p. 176-84.
5. Kobata H, Kondo A, Iwasaki K, Kusaka H, Ito H, Sawada S. Chordoid meningioma in a child: case report. *J Neurosurg* 1998 : 88 ; 319-23.
6. Glasier CM, Husain MM, Chaddock W, Boop FA. Meningiomas in children: MR and histopathologic findings. *AJNR Am J Neuroradiol* 1993 : 14 ; 237-41.
7. Civit T, Baylac F, Taillandier L, Auque J, Hepner H. Chordoid meningiomas. Clinical, neuroradiological and anatomopathological aspects. Apropos of a new case and review of the literature. *Neurochirurgie* 1997 : 43 ; 308-13.
8. Kajiwara Y, Kodama Y, Hotta T, Kohno H, Taniguchi E, Yamasaki F, et al. A case of chordoid meningioma. *No Shinkei Geka* 1999 : 27 ; 947-51.
9. Soo MY, Ng T, Gomes L, Da Cruz M, Dexter M. Skull base chordoid meningioma: imaging features and pathology. *Australas Radiol* 2004 : 48 ; 233-6.
10. Salinero E, Beltran L, Costa JR. Intraoperative cytologic diagnosis of chordoid meningioma: a case report. *Acta Cytol* 2004 : 48 ; 259-63.
11. Inagawa H, Ishizawa K, Shimada S, Shimada T, Nishikawa R, Matsutani M, et al. Cytologic features of chordoid meningioma: a case report. *Acta Cytol* 2004 : 48 ; 397-401.
12. Zuppan CW, Liwnicz BH, Weeks DA. Meningioma with chordoid features. *Ultrastruct Pathol* 1994 : 18 ; 29-32.
13. Abenzoa P, Sibley RK. Chordoma: an immunohistologic study. *Hum Pathol* 1986 : 17 ; 744-7.
14. Mierau GW, Weeks DA. Chondroid chordoma. *Ultrastruct Pathol* 1987 : 11 ; 731-7.
15. Cybulski GR, Russell EJ, D'Angelo CM, Bailey OT. Falcine chondrosarcoma: case report and literature review. *Neurosurgery* 1985 : 16 ; 412-5.
16. Martin RF, Melnick PJ, Warner NE, Terry R, Bullock WK, Schwinn CP. Chordoid sarcoma. *Am J Clin Pathol* 1973 : 59 ; 623-35.
17. Nora FE, Scheithauer BW. Primary epithelioid heman-gioendothelioma of the brain. *Am J Surg Pathol* 1996 : 20 ; 707-14.
18. Radner H, Katenkamp D, Reifenberger G, Deckert M, Pietsch T, Wiestler OD. New developments in the pathology of skull base tumors. *Virchows Arch* 2001 : 438 ; 321-35.
19. Brat DJ, Scheithauer BW, Staugaitis SM, Cortez SC, Brecher K, Burger PC. Third ventricular chordoid glioma: a distinct clinicopathologic entity. *J Neuropathol Exp Neurol* 1998 : 57 ; 283-90.
20. Karamitopoulou E, Perentes E, Tolnay M, Probst A. Prognostic significance of MIB-1, p53, and bcl-2 immunoreactivity in meningiomas. *Hum Pathol* 1998 : 29 ; 140-5.
21. Aguiar PH, Agner C, Simm R, Freitas AB, Tsanaclis AM, Plese P. p53 Protein expression in meningiomas: a clinicopathologic study of 55 patients. *Neurosurg Rev* 2002 : 25 ; 252-7.
22. Matsuno A, Nagashima T, Matsuura R, Tanaka H, Hirakawa M, Murakami M, et al. Correlation between MIB-1 staining index and the immunoreactivity of p53 protein in recurrent and non-recurrent meningiomas. *Am J Clin Pathol* 1996 : 106 ; 776-81.
23. Perry A, Stafford SL, Scheithauer BW, Suman VJ, Lohse CM. The prognostic significance of MIB-1, p53, and DNA flow cytometry in completely resected primary meningiomas. *Cancer* 1998 : 82 ; 2262-9.
24. Amatya VJ, Takeshima Y, Sugiyama K, Kurisu, K, Nishisaka T, Fukuhara T, et al. Immunohistochemical study of Ki-67 (MIB-1), p53 protein, p21WAF1, and p27KIP1 expression in benign, atypical, and anaplastic meningiomas. *Hum Pathol* 2001 : 32 ; 970-5.
25. Korshunov A, Shishkina L, Golanov A. Immunohistochemical analysis of p16INK4a, p14ARF, p18INK4c, p21CIP1, p27KIP1 and p73 expression in 271 meningiomas correlation with tumor grade and clinical outcome. *Int J Cancer* 2003 : 104 ; 728-34.
26. Andersson U, Guo D, Malmer B, Bergenheim AT, Brannstrom T, Hedman H, et al. Epidermal growth factor receptor family (EGFR, ErbB2-4) in gliomas and meningiomas. *Acta Neuropathol (Berl)* 2004 : 108 ; 135-42.
27. Steilen-Gimbel H, Niedermayer I, Feiden W, Freiler A, Steudel WI, Zang KD, et al. Unbalanced translocation t(1; 3)(p12-13; q11) in meningiomas as the unique feature of chordoid differentiation. *Genes Chromosomes Cancer* 1999 : 26 ; 270-2.
28. Leone PE, Bello MJ, de Campos JM, Vaquero J, Sarasa JL, Pestana A, et al. NF2 gene mutations and allelic status of 1p, 14q and 22q in sporadic meningiomas. *Oncogene* 1999 : 18 ; 2231-9.
29. Bostrom J, Muhlbauer A, Reifenberger G. Deletion mapping of the short arm of chromosome 1 identifies a common region of deletion distal to D1S496 in human meningiomas. *Acta Neuropathol (Berl)* 1997 : 94 ; 479-85.
30. Bello MJ, de Campos JM, Kusak ME, Vaquero J, Sarasa

- JL, Pestana A, et al. Allelic loss at 1p is associated with tumor progression of meningiomas. *Genes Chromosomes Cancer* 1994 ; 9 ; 296-8.
31. Pfisterer WK, Hank NC, Preul MC, Hendricks WP, Puschel J, Coons SW, et al. Diagnostic and prognostic significance of genetic regional heterogeneity in meningiomas. *Neuro-oncol* 2004 ; 6 ; 290-9.
32. Weber RG, Bostrom J, Wolter M, Baudis M, Collins VP, Reifenberger G, et al. Analysis of genomic alterations in benign, atypical, and anaplastic meningiomas : toward a genetic model of meningioma progression. *Proc Natl Acad Sci USA* 1997 ; 94 ; 1719-24.
33. Lamszus K, Kluwe L, Matschke J, Meissner H, Laas R, Westphal M. Allelic losses at 1p, 9q, 10q, 14q, and 22q in the progression of aggressive meningiomas and undifferentiated meningeal sarcomas. *Cancer Genet Cytogenet* 1999 ; 110 ; 103-10.